Journal of Energy Storage 86 (2024) 111246

Contents lists available at ScienceDirect

Journal of Energy Storage

journal homepage: www.elsevier.com/locate/est

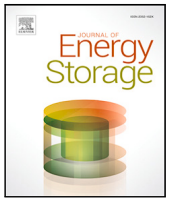

Research papers

Optimal hybrid power dispatch through smart solar power forecasting and battery storage integration

Keaobaka D. Poti [a], Raj M. Naidoo [a], Nsilulu T. Mbungu [b,c,*], Ramesh C. Bansal [c,a]

[a] Department of Electrical, Electronics and Computer Engineering, University of Pretoria, Pretoria, South Africa
[b] Department of Electrical Engineering, Tshwane University of Technology, Pretoria, South Africa
[c] Department of Electrical Engineering, University of Sharjah, Sharjah, United Arab Emirates

ARTICLE INFO

Keywords:
Battery storage
Commercial sectors
Demand management
Forecasting
Optimization
PV power plants
System planning

ABSTRACT

This study presents a strategy to optimize hybrid power system dispatch for commercial sectors in South Africa while utilizing the day-ahead method to forecast solar photovoltaic (PV) power. The approach utilizes numerical weather prediction (NWP) models obtained from open weather maps and incorporates power plant specifications to generate predictions of the PV power plant's output. These predictions are then integrated into an optimal control strategy incorporating battery storage. The use of optimal algorithms helps manage PV power plant curtailment during periods of over-generation. It is crucial to optimize PV power systems and ensure a continuous power supply for solar power plants, even during unfavorable weather conditions. Besides, the study develops a model that solves the challenging questions of combining solar power forecasting with an optimal dispatch and demand management scheme. Therefore, there is a need to incorporate battery storage systems through the developed optimal control method to maximize the energy from the PV system and minimize the power from the utility grid. The obtained results demonstrate the effectiveness of the developed model. The winter season presented a lower MAE of 21 kW, an RMSE of 35.4 kW, and a MAPE of 3,1% for PV power output forecasting, showing that the errors during prediction are lower compared to other seasons. It has been observed that 60% of the load is supplied through a combination of PV power and battery storage. Therefore, evidence of the developed optimal hybrid power dispatch with an innovative solar power forecasting model suggests that accurate forecasting can improve system planning and mitigate the necessity of procuring grid power at high electricity prices.

1. Introduction and literature review

The global penetration rates of photovoltaic (PV) systems are clearly on the rise, as indicated by the International Energy Agency (IEA) reporting a 22% increase in solar PV generation in 2021, resulting in over 1000 TWh of energy production [1]. This shift away from conventional power sources is supported by ongoing policy developments within the energy sector [2–6]. Recent advancements include the implementation of carbon tax policies, feed-in tariffs, and payback schemes, all aimed at incentivizing the adoption of renewable energy sources. Furthermore, the integration of renewable energy into the economy is viewed as both a sustainable economic stimulus and a vital requirement for achieving net-zero targets [7,8]. It is also anticipated that utility-scale PV systems, along with wind power, will continue to experience a steady increase in capacity penetration [9].

The overall costs of solar energy have become more competitive and cost-effective, contributing to its continued deployment despite potential declines in value [10–13]. While renewable energy sources have made distribution systems cleaner and more environmentally friendly, they have introduced inherent variability and complexity, leading to power supply instability. To effectively manage the power supply and the stochastic nature of PV generation, extensive research has been conducted on the use of battery storage systems [14–19]. Furthermore, as renewable energy accounts for a larger share of grid capacity, the risk of curtailment is projected to increase significantly [20,21]. To address this challenge, alternative contract structures and methods have been developed to reallocate potentially curtailed energy and risk [22–25].

The rapid growth of renewable energy capacity worldwide has underscored the importance of accurate power generation forecasting to ensure effective power system management and grid balancing [26–29]. Given the inherent variability and limited predictability of wind and solar resources, precise forecasting plays a central role in minimizing uncertainty and supporting optimal decision-making

* Corresponding author at: Department of Electrical Engineering, Tshwane University of Technology, Pretoria, South Africa.
E-mail address: ntmbungu@ieee.org (N.T. Mbungu).

https://doi.org/10.1016/j.est.2024.111246
Received 12 July 2023; Received in revised form 30 December 2023; Accepted 8 March 2024
Available online 22 March 2024

Nomenclature

Parameters and constants

ANN	Artificial neural network
BESS	Battery energy storage system
GHI	Global horizontal irradiance
IEA	International Energy Agency
MAE	Mean absolute error
MPC	Model predictive control
NAM	North American Mesoscale Forecast System
NOCT	Normal operating cell temperature
NREL	Renewable energy laboratory
NWP	Numerical weather prediction
OEDI	Open energy data initiative
PV	Photovoltaic
RMSE	Root mean square error
SMPC	Stochastic model predictive control
STC	Standard testing conditions

for planners and operators [30]. However, the accuracy of existing forecasting methods remains a concern, as inaccurate forecasts can lead to substantial financial losses for utilities [31,32]. Moreover, forecast accuracy significantly impacts the revenue optimization of PV plus battery power plants in day-ahead energy markets [33]. To improve PV power forecasting accuracy, numerous methods have been researched and developed, with machine learning models emerging as the most recent and widely utilized approach [34,35]. Additionally, numerical weather prediction (NWP) methods are being developed in conjunction with machine learning techniques.

The role of solar irradiance forecasting in the planning and operation of power systems with high solar power generation penetration was discussed in [27]. Wang et al. conducted a study on the costs associated with day-ahead solar forecast errors across 667 existing solar power plants in the United States [36]. The study analyzed two types of solar forecasts, namely persistence forecasts and numerical weather prediction forecasts, focusing on the years 2012 to 2019. The research highlighted the costs associated with forecast errors at different solar power plants, revealing that North American mesoscale forecast system (NAM) forecast errors had relatively low costs, averaging no more than $1/MWh in most years.

Tawn and Browell provided an up-to-date overview of established and emerging approaches in the field of very short-term wind and solar forecasting [30]. The review explored the transfer of knowledge between wind and solar forecasting and identified new opportunities, particularly in the use of remote sensing technology. In [37], an ensemble-based k-nearest neighbor algorithm was developed for wind and solar power forecasting. The study utilized the Makowski metric analysis for training and optimizing the k-nearest neighbor algorithm, and the chi-square distance was employed to assess the goodness of fit between expected and observed values. Gorman et al. investigated the resilience benefits of behind-the-meter solar-plus-storage systems for residential customers [38]. The study revealed that systems with 10 kWh of storage could meet critical loads in most counties in the United States throughout the year. However, when heating and cooling loads were considered critical, the capability of meeting critical loads dropped to an average of 86% across all counties and months. Abdelghany et al. presented a control strategy to enhance the reliability and commercialization of energy storage systems within microgrids [39]. The study employed a scenario-based approach to implement the stochastic model predictive control (SMPC) strategy for the energy management of grid-connected hybrid energy storage systems.

Syed and Khalid proposed a novel neural network model predictive control (MPC) approach that utilized a neural network model of the plant for photovoltaic power smoothing with battery energy storage [40]. The study demonstrated that the proposed controller significantly reduced battery charging levels and state of charge compared to fuzzy logic controllers.

Notably, most research in this field tends to focus exclusively on PV power forecasting, often neglecting the integration of these forecasts with energy demand management and optimal power dispatch strategies for commercial buildings in an innovative grid environment. Battery storage systems are often used exclusively for peak shifting rather than PV power optimization [41]. Therefore, this study identifies the need to integrate a smart forecasting method with a solar PV power system in commercial sectors, as well as the integration of an optimal control strategy for the PV system power output, such as battery storage, with forecasting techniques. With South Africa, among other countries, emphasizing the expansion of renewable energy sources, particularly solar and wind power, accurate forecasting becomes crucial. Thus, the research aims to address the problem of accurately forecasting solar energy production to effectively manage solar power variability and improve optimization and availability of solar PV energy during high load levels in commercial sectors.

This contribution aligns with the following objectives:

- Developing a day-ahead forecasting method tailored for commercial applications, focusing on solar PV power. Thus, this approach recognizes the unique requirements and challenges faced by commercial applications in South Africa, taking into account factors such as load variations, energy demands, and market dynamics
- Conducting research to devise an optimal control strategy that enhances the reliability and availability of a solar power plant by integrating a battery storage system. This integration allows for better management of PV power curtailment during periods of over-generation and ensures a continuous power supply, even during unfavorable weather conditions.
- Improving the balance between demand and supply by utilizing the proposed forecasting model for accurate power prediction. Thus, the study aims to minimize imbalances between consumers and suppliers, leading to more efficient energy utilization and reduced reliance on the grid. Besides, this study seeks to optimize the dispatch of hybrid power systems in commercial sectors by developing a day-ahead forecasting method, implementing an optimal control strategy with battery storage integration, and utilizing accurate power prediction for improved demand and supply management.

The remaining part of this research study can be summarized as follows: Section 2 presents the proposed model approach and development. Section 3 presents the data collected to conduct an analysis of the proposed forecasting and integration model. In Section 4, results and discussions, performance evaluation of the model and hybrid dispatch optimization are presented. Sections Section 5 gives a conclusion of the work presented as well as some recommendations for future work.

2. Model approach and development

2.1. Proposed approach

The forecasting model incorporates weather forecasts obtained from online sources, along with the specifications of the solar panels. By combining these inputs, the model aims to forecast the output of a PV system without relying on historical data specific to that particular PV system. This approach ensures that PV systems without historical data can still utilize the model for effective power planning. In this research, the exclusion of certain weather parameters beyond ambient temperature, solar irradiance, and wind speed is attributed to the focus on a specific set of factors relevant to the study's objectives. The decision to narrow the scope was made to streamline the analysis and

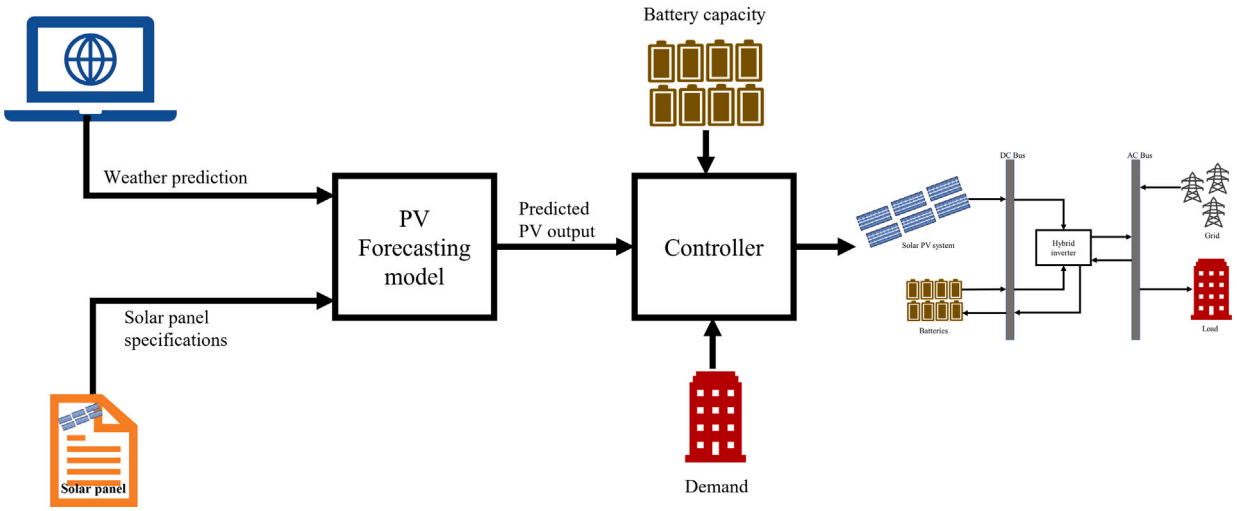

Fig. 1. Forecasting model approach with an optimal hybrid power dispatch.

maintain a clear focus on the primary variables influencing PV power forecasting, thereby ensuring precision and coherence in the research outcomes [42]. Fig. 1 demonstrates how the forecasting model will be integrated into the hybrid power system, utilizing optimal control methods to optimize the system's performance. The focus of this model is on commercial applications, where the solar PV system, battery energy storage system (BESS), and grid collectively supply power to a commercial load. While the commercial load remains connected to the grid, the objective is to maximize the utilization of power from the PV system and minimize dependence on the grid, taking into account various factors that influence the PV system's output.

2.2. Model development

2.2.1. Cell temperature modeling

According to [43], the basic linear equation representing cell efficiency as a function of cell temperature is as follows:

$$\eta_{cell} = \eta_{T,stc}[1 - \beta_{stc}(T_c - T_{c,stc})] \tag{1}$$

η_{cell} is the cell efficiency, $\eta_{T,stc}$ is the electrical efficiency of the cell at STC, β_{stc} is the temperature coefficient depending on the material used for the cell, and $T_{c,stc}$ is the cell temperature at STC. The cell operating temperature is represented by T_c. The cell temperature can be calculated at normal operating cell temperature (NOCT). NOCT is defined as cell temperature that is reached when modules are exposed to a nominal thermal environment at wind speeds of 1 m/s, an ambient temperature of 20 °C, and solar radiation levels of 800 W/m^2. NOCT values typically range from 30 °C to 45 °C on module nameplates. To calculate T_c three different functions will be tested. The first function is the standard approach which takes into account NOCT based on the technology used. T_c is calculated as follows [44]:

$$T_c = T_a + \frac{G}{G_{NOCT}}(T_{NOCT} - T_{a,NOCT}) \tag{2}$$

The ambient temperature at NOCT $T_{a,NOCT}$ is 20 °C. For the purpose of the model a typical T_{NOCT} of 45 °C is assumed for all technologies. The next T_c approach takes into account wind speeds that would be measured near the modules. The cell temperature model which is described as a simple empirical model is calculated as follows [45]:

$$T_c = T_a + \frac{G}{W_1.v_w + W_o} \tag{3}$$

where W_1 and W_o are constants and are specified for different PV technologies. v_w is the wind speed, G is the global horizontal irradiance (GHI), and T_a is the ambient temperature. Another approach to calculate T_c that was previously proposed and will be used to calculate T_c is modeled as [46]:

$$T_c = \frac{U_{pv}(v).T_a + G[\tau.\alpha - \eta_{STC}(1 - \beta_{STC}.T_{STC})]}{U_{pv}(v) + \beta_{STC}.\eta_{STC}.G} \tag{4}$$

$U_{pv}(v)$ is the module's total surface heat exchange coefficient. The heat exchange coefficient can be represented as a function of the wind speed that can be measured closer to the module. $\tau.\alpha$ was calculated at 0.81. The heat exchange coefficient can be represented as [47]:

$$U_{pv}(v_w) = 24.1 + 2.9v_w \tag{5}$$

2.2.2. PV output power forecasting equation

The proposed solar power output forecasting model is shown in Fig. 2. This model leverages real-world data by combining weather predictions with PV system specifications to generate real-time forecasts. To forecast the daily output power, the hourly output power will first be calculated, and the 24-h output summed. This is to ensure that discrepancies or errors between the measured and forecasted model are minimized by not taking the daily average weather forecast.

The equation to forecast the output power ($P_{o,daily}$) of the PV system can be calculated as follows:

$$P_{o,daily} = P_o(1) + P_o(2) + P_o(3) + P_o(4) + \cdots + P_o(24) \tag{6}$$

$$P_{o,daily} = \sum_{t=1}^{24} P_o(t) \tag{7}$$

The hourly output power can be calculated as [42,48]:

$$P_o(t) = P_{o,stc} \times \frac{G}{G_{stc}} \times [1 + \gamma_{stc}(T_c - T_{c,stc})] \times Z_{pv} \tag{8}$$

Z_p is the configuration of the PV panels. The configuration of the PV panels can be further expressed as:

$$Z_{pv} = N_p \times N_s, \tag{9}$$

where N_p and N_s express the number of PV panels in parallel and the number of PV panels in series respectively.

2.2.3. Hybrid power system dispatch

As per the selected sequence for this research, the PV-generated power will be dispatched first to meet the load. The equation governing the PV dispatch is:

$$P_{load,remaining} = P_{load} - P_{PV} \tag{10}$$

P_{load} is the load demand, P_{PV} is the power supplied by PV to the load, and $P_{load,remaining}$ load is the unmet load after the PV power has

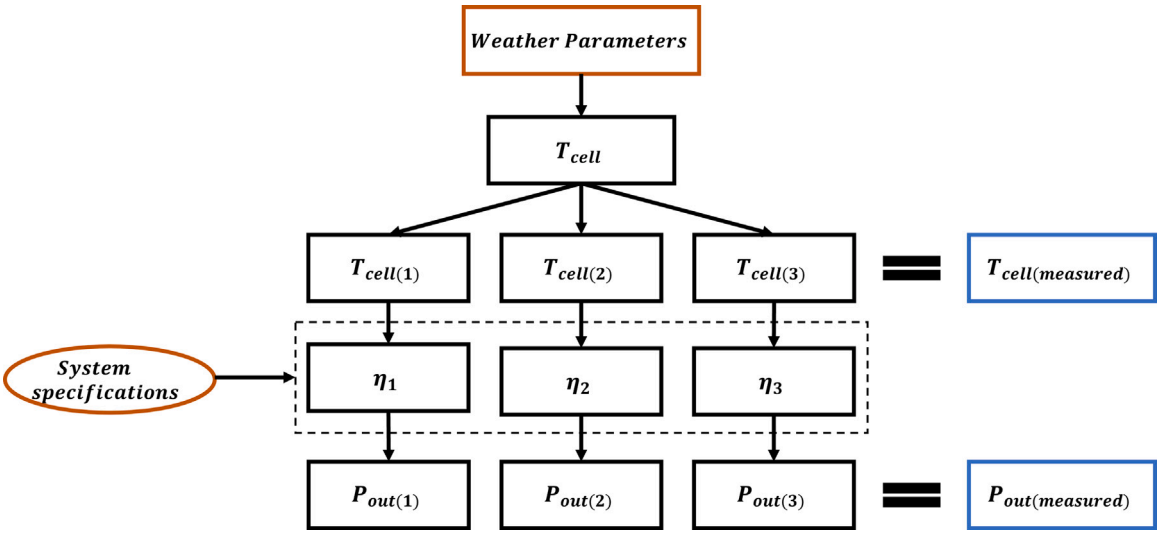

Fig. 2. Approach to be implemented in this research.

been dispatched. Next, the battery P_{bat} will be charged or discharged depending on whether the load was fully met by the dispatched PV power. The remaining load is governed by the following equation:

$$P_{load,remaining} = P_{load} - P_{PV} \pm P_{bat} \tag{11}$$

P_{bat} state of charge or discharge will be dependent on the following conditions:

$$P_{bat} = \begin{cases} 0, & P_{load,remaining} = 0. \\ +P_{bat}, & P_{load,remaining} < 0. \\ -P_{bat}, & P_{load,remaining} > 0 \end{cases} \tag{12}$$

The battery would be charged if $P_{load,remaining} < 0$ as that would mean the PV generated power was in excess. In the same logic, $P_{load,remaining} > 0$ would mean that the load was not met by the dispatched PV power and the battery would then be discharged. The battery's state of charge determines the available power to be discharged, as well as the remaining battery power to charge it.

Finally, the grid power P_{grid} will be dispatched only if the required load is still unmet after the PV power is dispatched and the battery discharged. Grid power will also be dispatched when there is no PV power available (typically at night and early morning) as the battery itself will not be able to meet the full load. $P_{l,rem}$ is then calculated as follows:

$$P_{l,rem} = P_{load} - P_{PV} \pm P_{bat} - P_{grid} \tag{13}$$

In the case of excess power dispatched where the load is met and the battery is fully charged, then the PV system will be curtailed. Fig. 3 shows the dispatch algorithm proposed.

2.2.4. Optimization model

The PV Module is represented as a variable power source from the sized PV plant. Operational costs of the PV plant are not considered for optimization. The battery is represented as a storage unit that is governed by a minimum state of charge and a maximum state of charge. For optimal sizing, it is assumed that the battery storage cost is included. The grid is modeled as a controllable power source and is governed by the net load demand after PV and battery dispatch. Since the building is in Pretoria as per assumptions, Tshwane Municipality tariffs will be considered. An optimization function *fmincon* in MATLAB, which solves constraint non-linear optimization problems will be used. The function is in the following format:

$$min f(x), \tag{14}$$

subject to

$$c(x) \leq 0, \tag{15}$$

$$c_{eq}(x) = 0, \tag{16}$$

$$A_{eq}(x) = b_{eq}, \tag{17}$$

$$lb \leq x \leq ub \tag{18}$$

where x is a vector of decision variables, f is a scalar-valued objective function, $c(x)$ is a vector of inequality constraints, and $c_{eq}(x)$ is a vector of equality constraints. A_{eq} and b_{eq} are linear equality constraints, where Aeq is a pxn matrix, and beq is a vector of length p. p is the number of equality constraints. ub and lb are the upper and lower bound constraints for the function. The economic hybrid dispatch model will therefore determine the optimal dispatch schedule to ensure that less PV is curtailed by sizing the BESS and that grid power is dispatched only when it is the cheapest energy source. Fig. 4 shows the flow to govern the objective function.

The objective function is subject to the following constraints:

$$P_{PV}(t) = P_1(t) + P_2(t) \tag{19}$$

$$P_L(t) = P_1(t) + P_3(t) + P_4(t) \tag{20}$$

$$SoC^{min} \leq SoC(t) \leq SoC^{max} (1 \leq t \leq N), \tag{21}$$

for all $t = 1, 2, \ldots .N$, where N is the number of hours in a day. $P_1(t)$ and $P_2(t)$ represent energy flows to the load and battery respectively, from the PV system. The energy flow from the battery is represented by $P_3(t)$ and the active power from the grid is represented by $P_3(t)$. The objective function is thus expressed as follows:

$$F = C_t \sum_{t=1}^{N} P_4(t), \tag{22}$$

where C_t is the electricity price at time t in \$/kWh. To calculate the battery capacity, the following expression is used:

$$B_c^{min} \leq B_c(0) + \eta_c \sum_{m=1}^{t} P_2(m) - \eta_d \sum_{m=1}^{t} P_3(m) \leq B_c^{max} \tag{23}$$

The battery capacity is represented by $B_c(t)$, where $B_c(0)$ is the initial state of charge, B_c^{min} is the minimum capacity level of the battery during discharge, and B_c^{max} is the maximum capacity level during charging stage. The charging and discharging efficiencies of the battery are represented by η_c and η_d respectively.

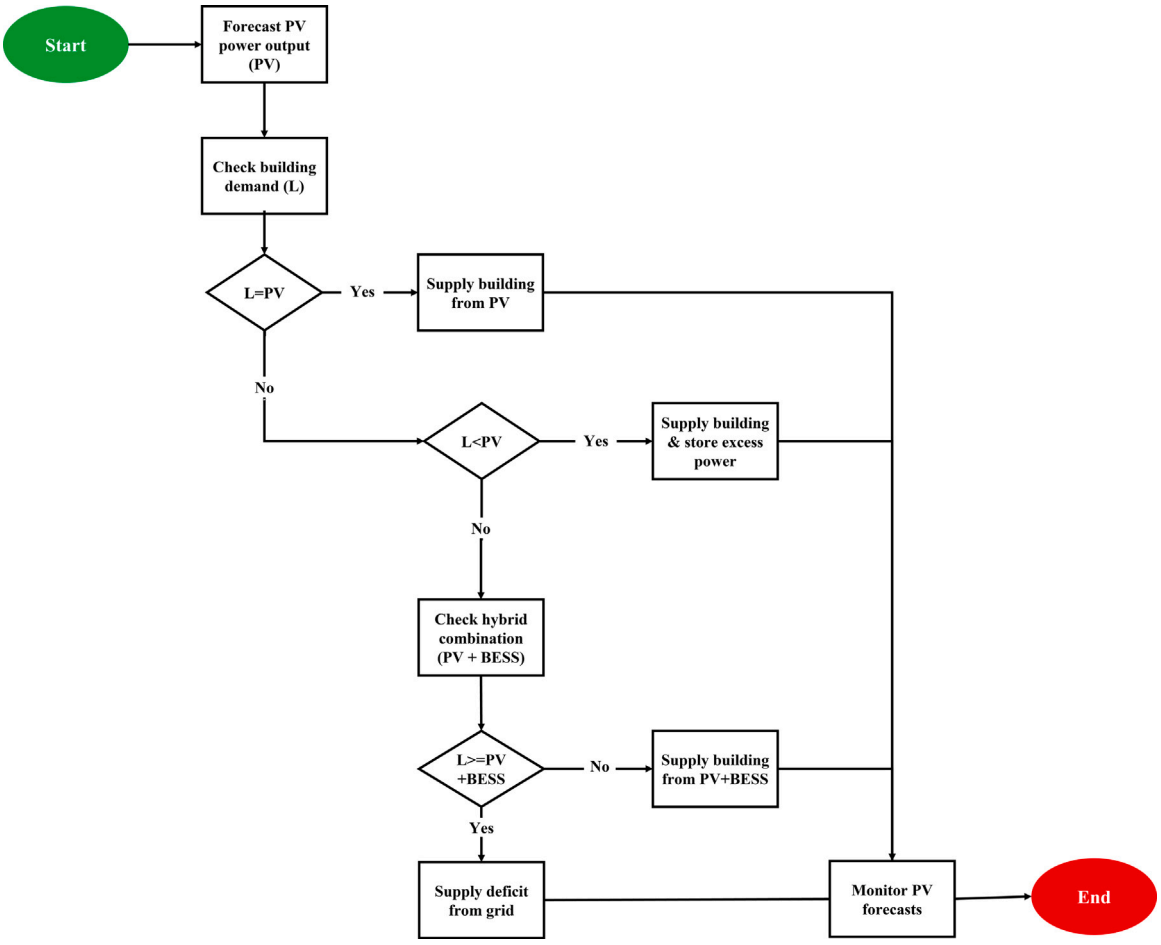

Fig. 3. Proposed dispatch control algorithm.

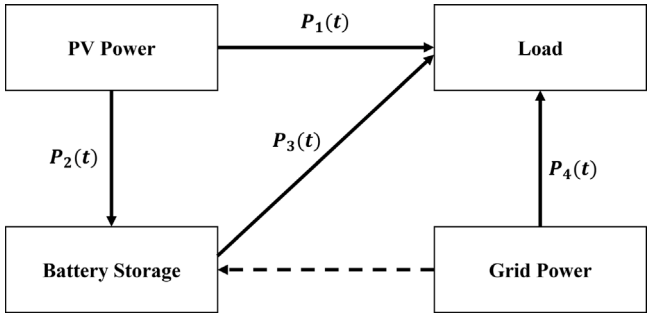

Fig. 4. Proposed dispatch control algorithm.

3. System assessment

3.1. Load demand: Consumer data

The proposed model aims to forecast the power output of a photovoltaic (PV) system to meet the energy needs of a commercial load. Specifically, we will analyze the load profile of a commercial office building. The dataset used for this analysis was obtained from the open energy data initiative (OEDI) website. In Figs. 5 and 6, we present the average load profile of the building over a 24-h period and a 744-h period, respectively.

The commercial energy demand can be characterized as follows:

- It operates as a commercial warehouse continuously from 12:00 AM to 11:59 PM.
- The facility requires a consistent and uninterrupted power supply throughout the day.
- Typical loads in the building include fans, cooling systems, lighting, and heating systems.

Based on the acquired data, we can assume a similar load profile for a large office building located in Pretoria, South Africa. This assumption is made due to the consistent and minimal fluctuations in demand observed across different seasons. The building exhibits an average power demand of 1360.17 kW and a peak power demand of 2153.1 kW.

3.2. Weather data

To predict PV output power, advanced weather forecasts are essential. As discussed previously, the primary weather data required for the proposed model are ambient temperature, irradiance, and wind speed. Two distinct weather sources, namely Open Weather Map (OWM) and Solcast, were used to acquire the necessary data points. OpenWeather Map is an online, web-based platform, offering access to historical, real-time, and forecasted weather data. The platform provides API keys, enabling real-time control of the forecasted output from the model. Similarly, the Solcast API toolkit, also web-based, delivers historical, live, and forecasted irradiance data, specifically designed to assist in PV power forecasting. Both weather sources used in this study leverage the numerical weather prediction (NWP) method to forecast day-ahead weather data.

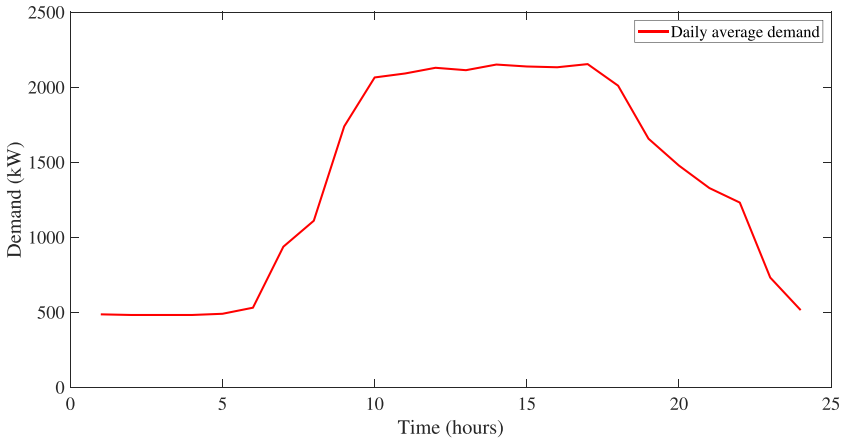

Fig. 5. Average daily load profile.

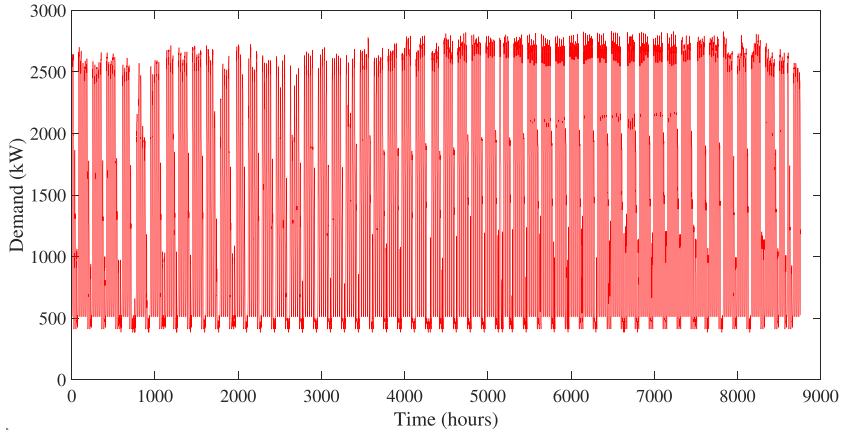

Fig. 6. Load profile over 8760 h.

3.3. Solar generation: PV plant data and system size

To determine the annual photovoltaic (PV) generation of the PV plant design, we conducted simulations using the PVWatts calculator tool developed by the National Renewable Energy Laboratory (NREL). The PVWatts calculator is an online tool specifically designed to estimate the energy production of grid-connected PV systems.

In Table 1, the monthly solar radiation data received in Pretoria, South Africa, is presented. It is worth noting that the average annual solar radiation in this location is 5.88 kWh/m^2/day. On-site measurements were obtained to compile the annual solar radiation data, as depicted in Fig. 7. With the assumed solar radiation level, a PV size of 5628.83 kW was obtained. To account for system inefficiencies and losses the PV system size selected is 5700 kW. Fig. 8 illustrates the annual PV output power generation from the designed PV plant, as calculated using the PVWatts simulator. The results provide insights into the expected energy production over a year.

Table 1
Monthly solar radiation received in Pretoria, South Africa [3].

Month	Solar radiation (kWh/m^2/day)
January	6.19
February	6.00
March	6.10
April	5.68
May	5.65
June	5.36
July	5.61
August	6.05
September	6.22
October	6.25
November	6.07
December	6.34
Annual	5.96

4. Results and discussion

4.1. PV output forecasting for the summer period

Fig. 9 presents the comparison between measured and predicted cell temperatures for a summer day, using three different cell temperature equations. Additionally, Fig. 10 illustrates the forecasted PV power output for the same day.

It is evident from Fig. 10 that there are minor disparities between the predicted and observed cell temperatures. These discrepancies can be attributed to abrupt variations in cloud cover, as the summer season in South Africa is known for its rainy weather.

Among the three cell temperature equations, Eq. (2) exhibits the least accurate prediction. It tends to overestimate cell temperature during the peak hour (12 PM) and fails to recognize sudden drops in irradiance. This equation solely considers GHI and ambient temperature, which proves to be a limitation during the summer period due to the frequent changes in cloud cover. Conversely, Eq. (4) yields the most accurate results compared to Eqs. (2) and (3). It demonstrates a strong forecasting capability with only minor deviations occurring after 3 PM.

Fig. 10 displays the forecasted PV power output obtained from the cell temperature equations for the summer day. Despite the observed

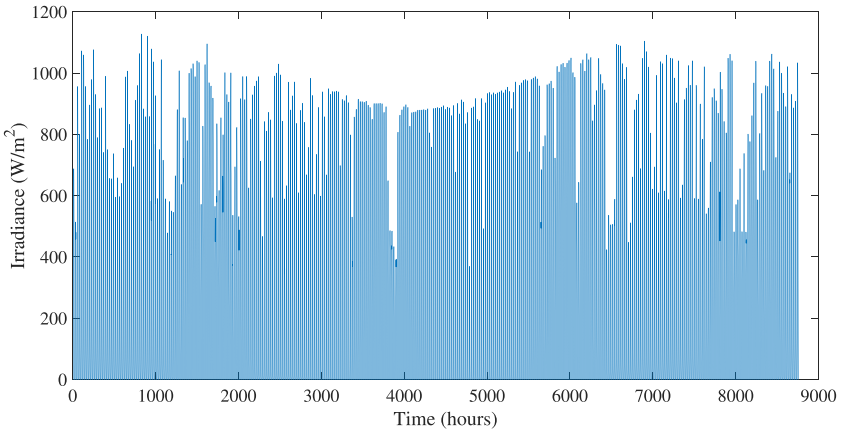

Fig. 7. Annual solar radiation obtained from the PV system site.

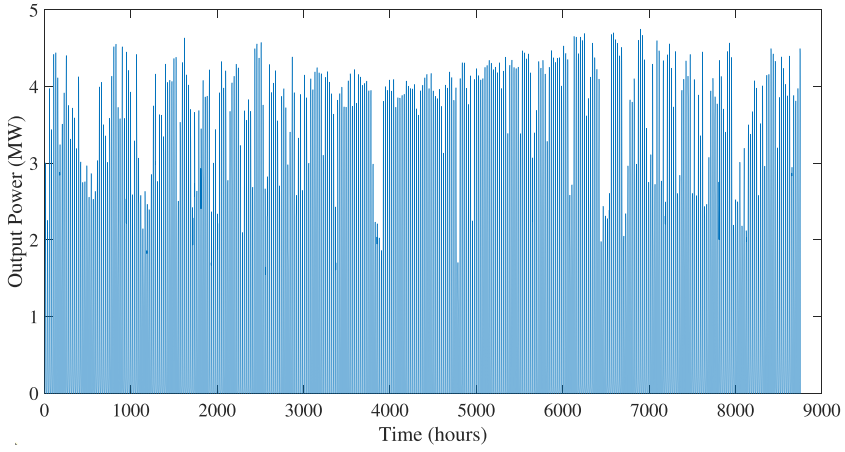

Fig. 8. Annual PV output power generation from the designed PV system.

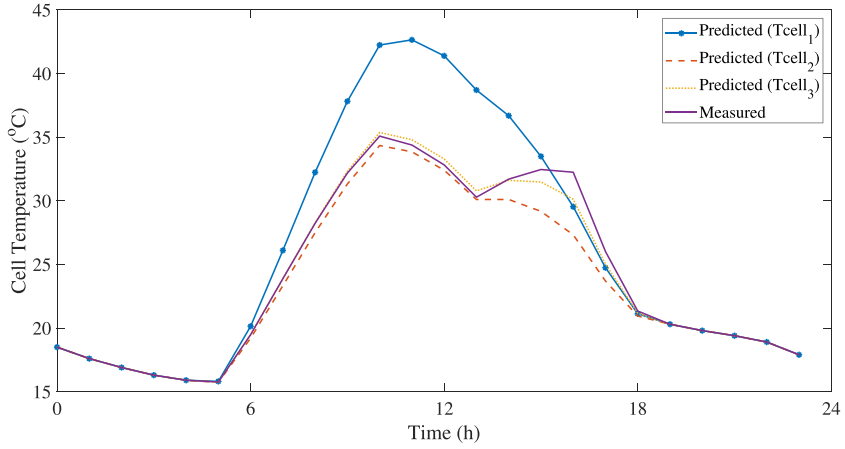

Fig. 9. Measured and predicted PV cell temperature for a day during summer.

deviations in the predicted cell temperature results, the model exhibits commendable forecasting capability. However, it should be noted that all three equations have slight shortcomings during the peak hours, where they tend to slightly overestimate the PV power output.

Fig. 11 illustrates the hourly comparison between predicted and measured cell temperatures during the summer period, which spans the months of December, January, and February in South Africa. The results reveal that Eq. (4) provides the most accurate predictions throughout the summer season, followed by Eq. (3). In contrast, Eq. (2) consistently exhibits mismatches between the predicted and measured cell temperatures, making it the least accurate equation for summer conditions. Notably, Eq. (2) tends to overestimate the cell temperature values.

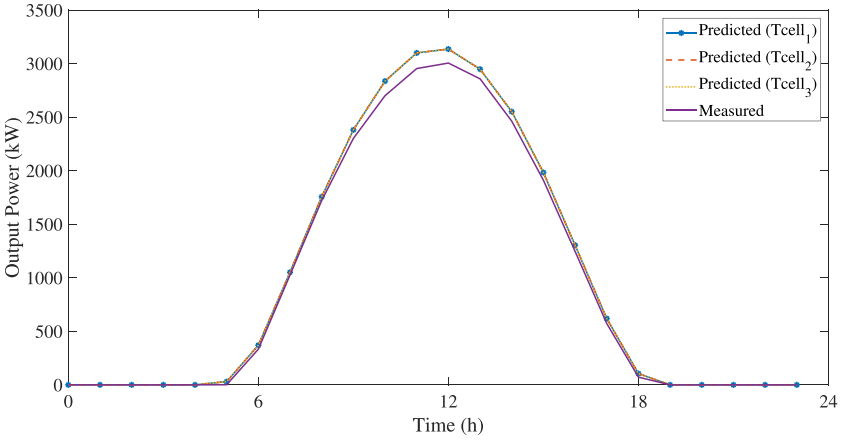

Fig. 10. Measured and predicted PV power output for a day in summer.

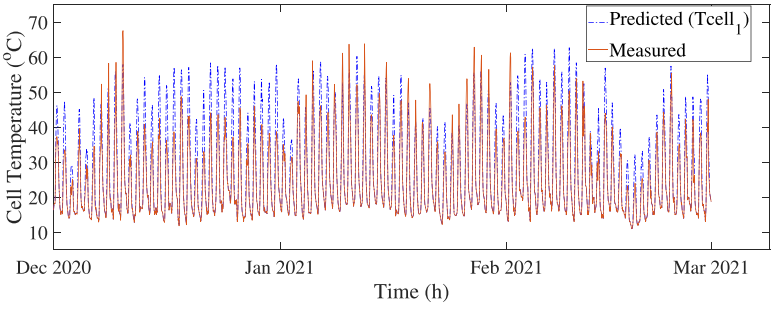

(a) Comparison between predicted and measured temperature for $cell_1$.

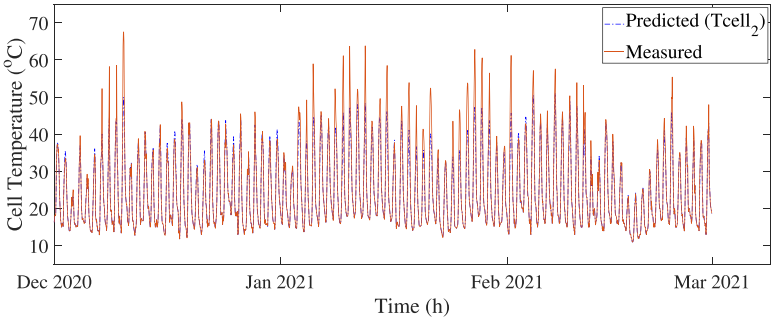

(b) Comparison between predicted and measured temperature for $cell_2$.

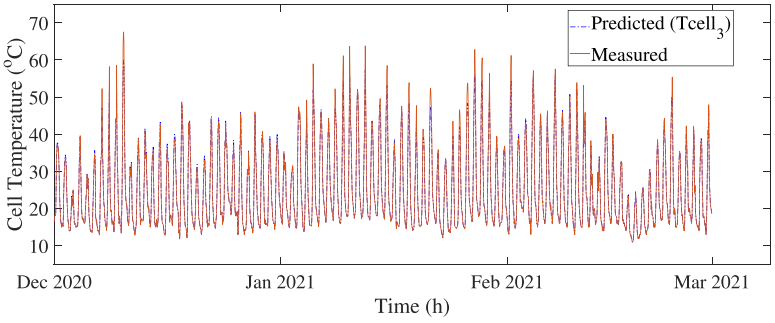

(c) Comparison between predicted and measured temperature for $cell_3$.

Fig. 11. Predicted and measured cell temperature for the summer season.

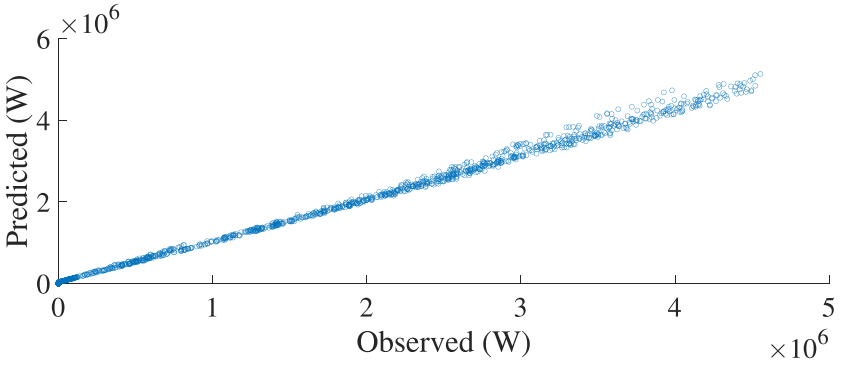

(a) Comparison between predicted and measured power for $cell_1$.

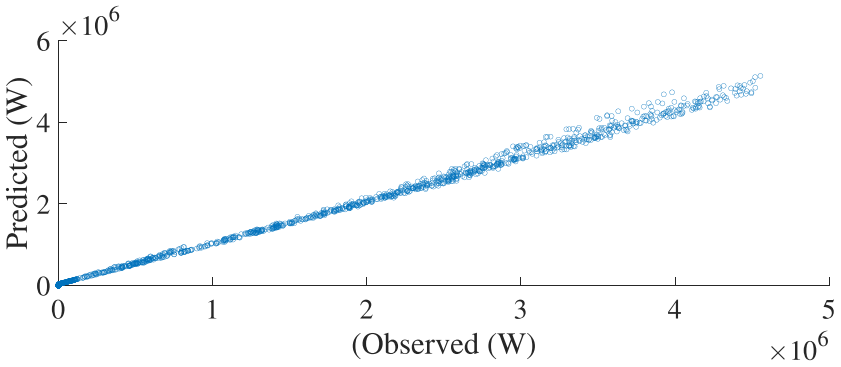

(b) Comparison between predicted and measured power for $cell_2$.

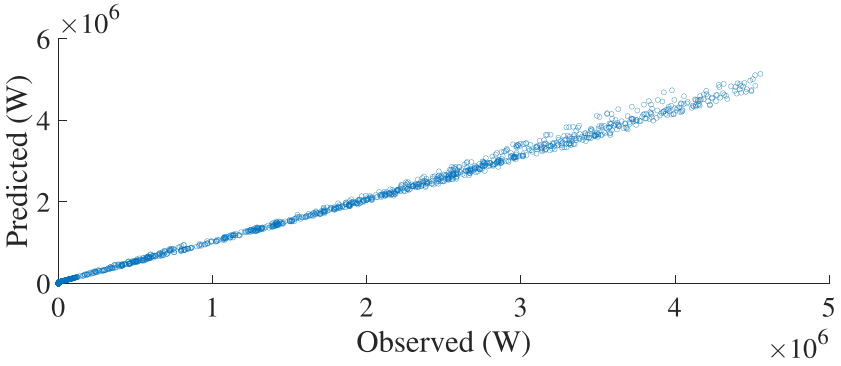

(c) Comparison between predicted and measured power for $cell_3$.

Fig. 12. Relationship between the predicted and observed PV output power during the summer.

From Fig. 11, the predicted and measured PV output power for the entire summer period can be determined using the methodology developed in Section 2.2. Although the three equations demonstrate reasonably accurate power forecasts for a specific day, the graph reveals slight inaccuracies persisting throughout the entire season. Notably, all three equations consistently tend to overestimate the output power, particularly during peak hours. This observation holds true across all three graphs, indicating a general tendency for over-prediction in the output power of the equations.

4.2. Performance evaluation

Fig. 12 provides a visual representation of the relationship between observed and predicted PV output power during the summer period. Figure also 12 demonstrates the model's favorable forecasting accuracy using the three equations. Despite the observed relationship between predicted and measured cell temperatures shown in Fig. 11, the model exhibits the capability to accurately forecast power output during the summer season.

Tables 2, 3, 4, and 5 offer a summary of the performance evaluation conducted for the predicted cell temperature for the different seasons. Subsequently, Tables 6, 7, 8, and 9 offer a summary of the performance evaluation conducted for the predicted output power for the different seasons. Among the three equations considered in this research, Tables 6, 7, 8, and 9 reveal that Eq. (4) yields the best overall prediction results.

For the summer period, the Mean Absolute Error (MAE) ranges between 41.89 kW and 41.97 kW, while the Root Mean Squared Error (RMSE) falls between 62.85 kW and 63 kW. The slightly higher RMSE compared to the MAE indicates the presence of larger errors in the predictions, contributing to the overall error. In conclusion, Eq. (4) demonstrates the best forecasting results among the equations considered.

4.3. Hybrid dispatch control optimization results

Fig. 13 illustrates the outcomes achieved through the optimal dispatch control, where the load demand is met by energy from the PV

Table 2
A summary of the predicted cell temperature model evaluation in summer.

Method	MAE (°C)	RMSE (°C)	MAPE (%)
Tcell1	2.2993	3.8295	7.3414
Tcell2	0.701	1.3805	2.3265
Tcell3	0.2609	0.5484	0.851

Table 3
A summary of the predicted cell temperature model evaluation in autumn.

Method	MAE (°C)	RMSE (°C)	MAPE (%)
Tcell1	3.4993	5.8061	10.7427
Tcell2	0.102	0.1795	0.3351
Tcell3	0.1964	0.3394	0.6014

Table 4
A summary of the predicted cell temperature model evaluation in winter.

Method	MAE (°C)	RMSE (°C)	MAPE (%)
Tcell1	1.9816	3.5218	6.3836
Tcell2	1.1232	2.1159	3.9067
Tcell3	0.2908	0.7326	1.105

Table 5
A summary of the predicted cell temperature model evaluation in spring.

Method	MAE (°C)	RMSE (°C)	MAPE (%)
Tcell1	5.2997	8,8598	13.7563
Tcell2	0.5035	0.9049	1.3143
Tcell3	0.3813	0.6564	0.9884

Table 6
A summary of the predicted PV output power model evaluation in summer.

Method	MAE (kW)	RMSE (kW)	MAPE (%)
Tcell1	41.8968	62.8510	194.4475
Tcell2	41.9894	63.0074	194.4543
Tcell3	41.9731	62.9839	194.4527

Table 7
A summary of the predicted PV output power model evaluation in autumn.

Method	MAE (kW)	RMSE (kW)	MAPE (%)
Tcell1	36.2888	64.8966	12.7511
Tcell2	36.4288	65.1535	12.7596
Tcell3	36.4200	65.1384	12.759

Table 8
A summary of the predicted PV output power model evaluation in winter.

Method	MAE (kW)	RMSE (kW)	MAPE (%)
Tcell1	21.0383	35.3705	3.1581
Tcell2	21.0925	35.4879	3.1610
Tcell3	21.0844	35.4637	3.1607

Table 9
A summary of the predicted PV output power model evaluation in spring.

Method	MAE (kW)	RMSE (kW)	MAPE (%)
Tcell1	70.7326	128.0966	7.5851
Tcell2	70.9712	128.5703	7.5972
Tcell3	70.9765	128.5832	7.5973

system, battery storage, and the grid. The total sources of power to supply the daily average load demand are presented in Fig. 13(a). From Fig. 13(b), it can be observed that the PV system supplies the load starting from 6:00 AM and continues until the peak load demand is reached around 6:00 PM, at which point it ceases to supply power. Subsequently, the battery storage discharges to meet the load demand from just after 4:00 PM until 9:00 PM, as depicted in 13(c). Finally, the grid power is utilized to supply the load from midnight (12:00 AM) until 7:00 AM, when the PV system resumes supplying power to the load, as shown in Fig. 13(d). Grid energy is again employed to supply the load from 8:00 PM until the remaining hours of the day.

Based on 13, it is evident that the PV power contributes the most to meeting the load demand. This significant contribution from the PV system can be attributed to the approach taken in sizing the PV system. With a peak load demand of 2.153 kW and a PV system size of 5700 kW, the PV system is adequately sized to meet the load demand, allowing for a higher contribution from PV power. Fig. 14 displays the energy flow on the battery storage during the charging and discharging process. Besides, the developed hybrid dispatch shows the distribution of the total contribution to the load demand among PV power, battery storage, and grid power. PV power accounts for 58% of the demand, and this contribution increases further when considering the energy transferred from the PV system to the battery. Battery energy storage contributes 24%, while the remaining 19% is sourced from the utility grid. Additionally, the developed model demonstrates that the dispatch of grid power is optimized by scheduling it during off-peak hours in the evening.

5. Conclusion

This research focused on solar PV power output forecasting using a day-ahead method. Three different methods were selected to model a day-ahead forecasting approach. The performance of the forecasting model was then evaluated across different weather seasons in South Africa, allowing for a comprehensive assessment of its effectiveness.

According to the findings presented in this study, Eq. (4) demonstrated the highest forecast accuracy among the three methods considered. This equation incorporates the heat exchange coefficient and wind speed, which are factors that impact forecasting accuracy. In contrast, Eq. (2), which only considers irradiance and ambient temperature, proved to be the least accurate due to its omission of other relevant weather variables.

It is highlighted that the model achieved the most accurate forecasts during the winter period, which can be attributed to the stable weather conditions experienced during that season. The winter season also exhibited lower errors in PV power output forecasting, with a Mean Absolute Error (MAE) of 21 kW, an RMSE of 35.4 kW, and a MAPE of 3.1%. These metrics indicate that the prediction errors were lower compared to other seasons.

It was demonstrated that 60% of the load was supplied by the combination of PV power and battery storage, showcasing the potential of accurate forecasting in improving system planning and avoiding the purchase of grid power at high electricity prices. However, it should be noted that the size of the battery storage, which was determined as 8.69 kW, did not take into account capital cost limitations and techno-economic evaluations, such as the payback period. This oversight could have financial implications for commercial buildings and render the investment in battery storage suboptimal. Future scope of work for this research will include the following:

- Using additional weather variables to develop a more accurate forecasting model for all seasons
- Conducting a thorough techno-economic assessment of the overall proposed optimal control algorithm
- Considering more local South African weather stations to develop an API integration suited to local requirements

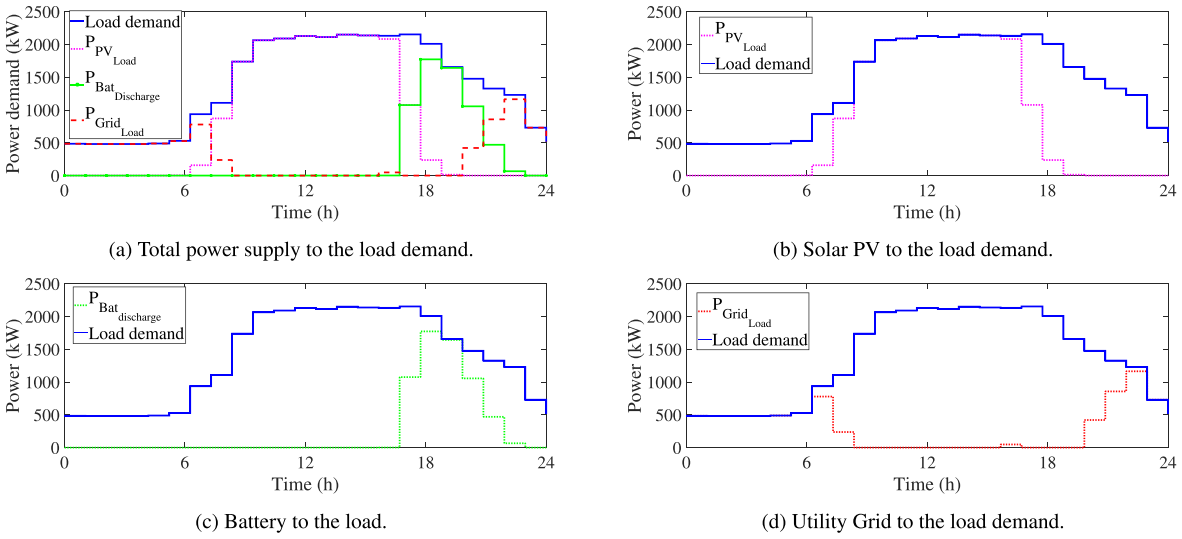

Fig. 13. Results of the optimal dispatch to load.

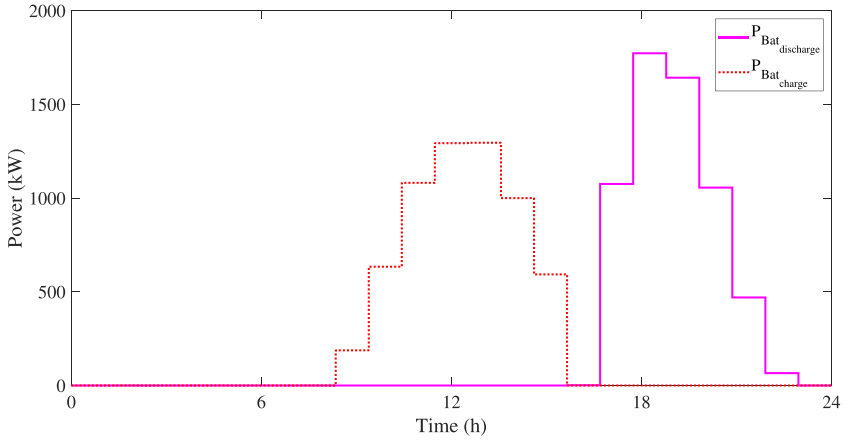

Fig. 14. Power flow in the battery energy storage.

CRediT authorship contribution statement

Keaobaka D. Poti: Conceptualization, Data curation, Formal analysis, Funding acquisition, Investigation, Methodology, Project administration, Resources, Software, Validation, Visualization, Writing – original draft, Writing – review & editing. **Raj M. Naidoo:** Conceptualization, Funding acquisition, Investigation, Methodology, Resources, Supervision, Validation, Visualization, Writing – review & editing. **Nsilulu T. Mbungu:** Conceptualization, Data curation, Formal analysis, Funding acquisition, Investigation, Methodology, Project administration, Resources, Software, Supervision, Validation, Visualization, Writing – original draft, Writing – review & editing. **Ramesh C. Bansal:** Conceptualization, Formal analysis, Funding acquisition, Investigation, Methodology, Resources, Supervision, Validation, Visualization, Writing – review & editing.

Declaration of competing interest

I would like to confirm that there are no potential conflicts of interest for this manuscript.

Data availability

Data will be made available on request.

Acknowledgment

The authors thank SANEDI for their funding contribution to the research.

References

[1] A. Jäger-Waldau, Snapshot of photovoltaics–February 2022, EPJ Photovolt. 13 (2022) 9.

[2] K. Kusakana, Optimal operation scheduling of grid-connected PV with ground pumped hydro storage system for cost reduction in small farming activities, J. Energy Storage 16 (2018) 133–138.

[3] N.T. Mbungu, R.M. Naidoo, R.C. Bansal, M.W. Siti, D.H. Tungadio, An overview of renewable energy resources and grid integration for commercial building applications, J. Energy Storage 29 (2020) 101385.

[4] IPCC, Summary for policymakers, in: V. Masson-Delmotte, P. Zhai, A. Pirani, S. Connors, C. Péan, S. Berger, N. Caud, Y. Chen, L. Goldfarb, M. Gomis, M. Huang, K. Leitzell, E. Lonnoy, J. Matthews, T. Maycock, T. Waterfield, O. Yelekçi, R. Yu, B. Zhou (Eds.), Climate Change 2021: The Physical Science Basis. Contribution of Working Group I To the Sixth Assessment Report of the Intergovernmental Panel on Climate Change, Cambridge University Press, Cambridge, United Kingdom and New York, NY, USA, 2021, pp. 3–32, http://dx.doi.org/10.1017/9781009157896.001.

[5] S. Potrč, L. Čuček, M. Martin, Z. Kravanja, Sustainable renewable energy supply networks optimization–the gradual transition to a renewable energy system within the European union by 2050, Renew. Sustain. Energy Rev. 146 (2021) 111–186.

[6] S.A.R. Khan, R.L. Ibrahim, A.Q. Al-Amin, Z. Yu, An ideology of sustainability under technological revolution: Striving towards sustainable development, Sustainability 14 (8) (2022) 4415.

[7] A.A. Ismail, N.T. Mbungu, A. Elnady, R.C. Bansal, A.-K. Hamid, M. AlShabi, Impact of electric vehicles on smart grid and future predictions: A survey, Int. J. Modell. Simul. 43 (6) (2023) 1041–1057.

[8] K. Kusakana, Optimal peer-to-peer energy management between grid-connected prosumers with battery storage and photovoltaic systems, J. Energy Storage 32 (2020) 101717.

[9] K. Nghitevelekwa, R. Bansal, A review of generation dispatch with large-scale photovoltaic systems, Renew. Sustain. Energy Rev. 81 (2018) 615–624.

[10] D. Millstein, R. Wiser, A.D. Mills, M. Bolinger, J. Seel, S. Jeong, Solar and wind grid system value in the United States: The effect of transmission congestion, generation profiles, and curtailment, Joule 5 (7) (2021) 1749–1775.

[11] Y. Zhang, M. Beaudin, R. Taheri, H. Zareipour, D. Wood, Day-ahead power output forecasting for small-scale solar photovoltaic electricity generators, IEEE Trans. Smart Grid 6 (2015) 2253–2262.

[12] R. Dubey, D. Joshi, R.C. Bansal, Optimization of solar photovoltaic plant and economic analysis, Electr. Power Compon. Syst. 44 (18) (2016) 2025–2035.

[13] R. Bansal, Handbook of Distributed Generation: Electric Power Technologies, Economics and Environmental Impacts, second ed., Springer, 2017.

[14] S. Samantaray, P. Kayal, Capacity assessment and scheduling of battery storage systems for performance and reliability improvement of solar energy enhanced distribution systems, J. Energy Storage 66 (2023) 107479.

[15] M. Krishnamoorthy, A.D.V.R. Periyanayagam, C. Santhan Kumar, B. Praveen Kumar, S. Srinivasan, P. Kathiravan, Optimal sizing, selection, and techno-economic analysis of battery storage for PV/BG-based hybrid rural electrification system, IETE J. Res. 68 (6) (2022) 4061–4076.

[16] K. Khalid Mehmood, S.U. Khan, S.-J. Lee, Z.M. Haider, M.K. Rafique, C.-H. Kim, Optimal sizing and allocation of battery energy storage systems with wind and solar power DGs in a distribution network for voltage regulation considering the lifespan of batteries, IET Renew. Power Gener. 11 (10) (2017) 1305–1315.

[17] C. Tang, J. Xu, Y. Sun, S. Liao, F. Zhang, L. Ma, Stochastic battery energy storage scheduling considering cell degradation and distributed energy resources, Int. Trans. Electr. Energy Syst. 29 (7) (2019) e12028.

[18] M. Azaroual, N.T. Mbungu, M. Ouassaid, M.W. Siti, M. Maaroufi, Toward an intelligent community microgrid energy management system based on optimal control schemes, Int. J. Energy Res. 46 (15) (2022) 21234–21256.

[19] T.B. Nkwanyana, M.W. Siti, Z. Wang, I. Toudjeu, N.T. Mbungu, W. Mulumba, An assessment of hybrid-energy storage systems in the renewable environments, J. Energy Storage 72 (2023) 108307.

[20] E. O'Shaughnessy, J.R. Cruce, K. Xu, Too much of a good thing? Global trends in the curtailment of solar PV, Sol. Energy 208 (2020) 1068–1077, http://dx.doi.org/10.1016/j.solener.2020.08.075.

[21] P. Denholm, J. Novacheck, J. Jorgenson, M. O'Connell, Impact of Flexibility Options on Grid Economic Carrying Capacity of Solar and Wind: Three Case Studies, Tech. rep., National Renewable Energy Lab.(NREL), Golden, CO (United States), 2016.

[22] E. O'Shaughnessy, J. Cruce, K. Xu, Rethinking solar PV contracts in a world of increasing curtailment risk, Energy Econ. 98 (2021) 105264.

[23] S.S. Ahmad, F.S. Al-Ismail, A.A. Almehizia, M. Khalid, Model predictive control approach for optimal power dispatch and duck curve handling under high photovoltaic power penetration, IEEE Access 8 (2020) 186840–186850.

[24] Z. Liu, Y. Du, Evolution towards dispatchable PV using forecasting, storage, and curtailment: A review, Electr. Power Syst. Res. 223 (2023) 109554.

[25] L.D. Bui, N.Q. Nguyen, B. Van Doan, E.R. Sanseverino, Forecasting energy output of a solar power plant in curtailment condition based on LSTM using P/GHI coefficient and validation in training process, a case study in Vietnam, Electr. Power Syst. Res. 213 (2022) 108706.

[26] N. Roy, P. Tripathy, S.C. De, B. Swargiary, S. Kumar, S. Das, N. Pathak, Day-ahead solar power generation forecasting using LSTM and random forest methods for North Eastern Region of India, in: 2022 22nd National Power Systems Conference, NPSC, IEEE, 2022, pp. 854–859.

[27] D. Yang, W. Wang, C.A. Gueymard, T. Hong, J. Kleissl, J. Huang, M.J. Perez, R. Perez, J.M. Bright, X. Xia, et al., A review of solar forecasting, its dependence on atmospheric sciences and implications for grid integration: Towards carbon neutrality, Renew. Sustain. Energy Rev. 161 (2022) 112348.

[28] R. Bansal, J. Pandey, Load forecasting using artificial intelligence techniques: a literature survey, Int. J. Comput. Appl. Technol. 22 (2–3) (2005) 109–119.

[29] D.P. Koottappillil, R.M. Naidoo, N.T. Mbungu, R.C. Bansal, Distribution of renewable energy through the energy internet: A routing algorithm for energy routers, Energy Rep. 8 (2022) 355–363.

[30] R. Tawn, J. Browell, A review of very short-term wind and solar power forecasting, Renew. Sustain. Energy Rev. 153 (2022) 111758.

[31] C. Chupong, B. Plangklang, Forecasting power output of PV grid connected system in thailand without using solar radiation measurement, 9, Elsevier Ltd, 2011, pp. 230–237, http://dx.doi.org/10.1016/j.egypro.2011.09.024,

[32] P. Mathiesen, C. Collier, J. Kleissl, A high-resolution, cloud-assimilating numerical weather prediction model for solar irradiance forecasting, Sol. Energy 92 (2013) 47–61, http://dx.doi.org/10.1016/j.solener.2013.02.018.

[33] R.A. Campos, G.L. Martins, R. Rüther, Assessing the influence of solar forecast accuracy on the revenue optimization of photovoltaic+ battery power plants in day-ahead energy markets, J. Energy Storage 48 (2022) 104093.

[34] D.P. Larson, L. Nonnenmacher, C.F. Coimbra, Day-ahead forecasting of solar power output from photovoltaic plants in the American southwest, Renew. Energy 91 (2016) 11–20, http://dx.doi.org/10.1016/j.renene.2016.01.039.

[35] S. Bimenyimana, G. Norense, O. Asemota, L. Lingling, L. Li, Output power prediction of photovoltaic module using nonlinear autoregressive neural network, J. Energy Environ. Chem. Eng. 2 (2017) 32–40, http://dx.doi.org/10.11648/j.jeece.20170204.11, URL http://www.sciencepublishinggroup.com/j/jeece.

[36] Y. Wang, D. Millstein, A.D. Mills, S. Jeong, A. Ancell, The cost of day-ahead solar forecasting errors in the United States, Sol. Energy 231 (2022) 846–856.

[37] T. Ahmad, S. Manzoor, D. Zhang, Forecasting high penetration of solar and wind power in the smart grid environment using robust ensemble learning approach for large-dimensional data, Sustainable Cities Soc. 75 (2021) 103269.

[38] W. Gorman, G. Barbose, J.P. Carvallo, S. Baik, C. Miller, P. White, M. Praprost, County-level assessment of behind-the-meter solar and storage to mitigate long duration power interruptions for residential customers, Appl. Energy 342 (2023) 121166.

[39] M.B. Abdelghany, A. Al-Durra, H. Zeineldin, F. Gao, Integrating scenario-based stochastic-model predictive control and load forecasting for energy management of grid-connected hybrid energy storage systems, Int. J. Hydrogen Energy (2023).

[40] M.A. Syed, M. Khalid, Neural network predictive control for smoothing of solar power fluctuations with battery energy storage, J. Energy Storage 42 (2021) 103014.

[41] M. Siti, N. Mbungu, D. Tungadio, B. Banza, L. Ngoma, R. Tiako, Economic dispatch in a stand-alone system using a combinatorial energy management system, J. Energy Storage 55 (2022) 105695.

[42] K.D. Poti, R.M. Naidoo, N.T. Mbungu, R.C. Bansal, Intelligent solar photovoltaic power forecasting, Energy Rep. 9 (2023) 343–352.

[43] E. Skoplaki, A. Boudouvis, J. Palyvos, A simple correlation for the operating temperature of photovoltaic modules of arbitrary mounting, Sol. Energy Mater. Sol. Cells 92 (11) (2008) 1393–1402.

[44] A. McEvoy, L. Castaner, T. Markvart, Solar Cells: Materials, Manufacture and Operation, Academic Press, 2012.

[45] M. Koehl, M. Heck, S. Wiesmeier, J. Wirth, Modeling of the nominal operating cell temperature based on outdoor weathering, Sol. Energy Mater. Sol. Cells 95 (7) (2011) 1638–1646.

[46] M. Mattei, G. Notton, C. Cristofari, M. Muselli, P. Poggi, Calculation of the polycrystalline PV module temperature using a simple method of energy balance, Renew. Energy 31 (4) (2006) 553–567.

[47] C. Schwingshackl, M. Petitta, J.E. Wagner, G. Belluardo, D. Moser, M. Castelli, M. Zebisch, A. Tetzlaff, Wind effect on PV module temperature: Analysis of different techniques for an accurate estimation, Energy Procedia 40 (2013) 77–86.

[48] Y. Riffonneau, S. Bacha, F. Barruel, S. Ploix, Optimal power flow management for grid connected PV systems with batteries, IEEE Trans. Sustain. Energy 2 (2011) 309–320, http://dx.doi.org/10.1109/TSTE.2011.2114901.